Instruction Manual for the Spectral Modelling of Three-Element Silicon Trap Detectors

Anna Vaskuri and Petri Kärhä
Metrology Research Institute, Aalto University

5 March 2019
Version 1.0

Contents

1   Introduction

This instruction manual explains all the steps needed for modelling the spectral responsivity of three element silicon trap detectors [1]. The spectral responsivity model is valid in the spectral range of 250 nm – 950 nm. The spectral responsivity of a trap detector is a combination of three terms: the ideal responsivity based on one photon creating one electron-hole pair, the reflectance of the detector, and the internal quantum efficiency of the photodiodes.

The theoretical background of the modelling is given in Chapter 2. Chapter 2.1 describes the spectral reflectance of an individual photodiode at different angles and polarizations, and the combined reflectance of a three-element trap detector, where a total of five reflections take place. Chapter 2.2 describes the model for internal quantum efficiency that is mainly dominated by loss mechanisms caused by trapped charges in the silicon dioxide layer grown on top of the silicon photodiode [1, 2]. In the ultraviolet region, below 400 nm, internal quantum efficiency is more complicated since the quantum yield starts affecting the results. This is explained in detail in Chapter 2.3.

The spectral responsivity model for a silicon trap detector has been implemented in Matlab program titled as *program_for_modelling_trap_responsivities_main_V1.m*. The structure and use of this program are described in Chapter 3. Chapter 3.1 gives instructions on how to use the program. Measurement data is given to the program in an Excel file, which also returns the modelled spectral responsivity. The structure of this file is described in Chapter 3.2. Chapter 3.3 gives Matlab source code of the program with its subprograms.

As input parameters, the model needs the experimental measurements of the silicon trap detector to be modelled: 1. Spectral responsivities at multiple laser wavelengths measured with a high-accuracy standard, such as a predictable quantum efficient detector (PQED) [3] or a cryogenic absolute radiometer [4], 2. Reflectances at multiple laser wavelengths, and 3. Spectral responsivity in the ultraviolet region 250 nm – 450 nm. Instructions for measuring these data are described in Chapter 4.

2   Spectral Responsivity Model

The spectral responsivity $R(\lambda)$ of a photodetector is defined as [5]

$$R(\lambda) = \frac{e\lambda}{hc} \cdot \epsilon_i'(\lambda) \cdot [1 - \rho(\lambda)], \tag{1}$$

where λ is the vacuum wavelength, e is the elementary charge, h is Planck constant, and c is the speed of light in vacuum. For an ideal photodiode each incident photon would create exactly one electron-hole pair as $R(\lambda) = e\lambda/hc$. In practice, the back reflection $\rho(\lambda)$ due to a significant refractive index change between air and the surface of a photodiode and the internal quantum efficiency $\epsilon_i'(\lambda)$ of a photodiode have to be taken into account. An example of the fitting of the spectral responsivity model in Eq. (1) to the experimental responsivity measurements of a trap detector at the Metrology Research Institute is presented in Fig. 1.
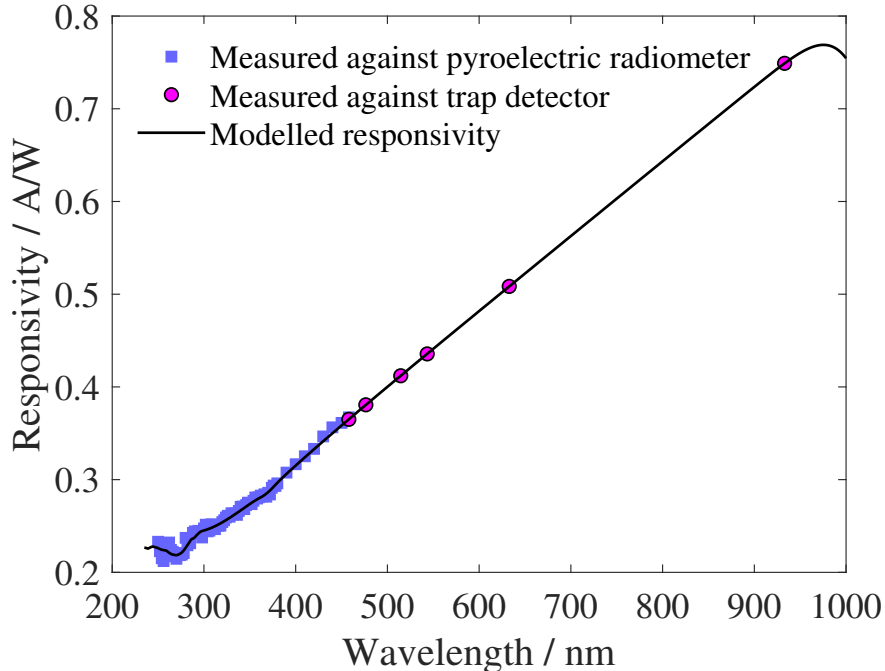
Figure 1: Spectral responsivity model in Eq. (1) fitted to the experimental responsivities of a three-element silicon trap detector.

The spectral reflectance $\rho(\lambda)$ of a silicon trap detector is measured at discrete wavelengths and then the spectral reflectance model is fitted to the experimental points with the thickness of a silicon dioxide layer as a free parameter. The modelling of the spectral reflectance and the fitting process are discussed in detail in Section 2.1.

The spectral internal quantum efficiency of a silicon photodiode from the ultraviolet to near infrared can be modelled as

$$\epsilon_i'(\lambda) = \eta(\lambda) \cdot \epsilon_i(\lambda), \tag{2}$$

where $\epsilon_i(\lambda)$ is the internal quantum efficiency in the visible and near-infrared wavelength

4

regions discussed in detail in Section 2.2 and $\eta(\lambda)$ is the quantum yield of silicon discussed in detail in Section 2.3, which exceeds unity in the ultraviolet wavelength region.

The algorithm fits the spectral responsivity model in Eq. (1) to the experimental responsivities using the *lsqnonlin* optimization function by custom-made Matlab software introduced in Section 3. There are three steps when fitting the spectral responsivity model to the experimental spectral responsivities. First, the spectral reflectance model is fitted to experimental reflectances of a trap detector. Second, the internal quantum efficiency is modelled in the visible and near-infrared wavelengths. Third, the quantum yield is modelled in the ultraviolet region. Table 1 lists free parameters to be fitted at each step by the relative least squares minimization method of a sum of the squared relative residuals

$$r_{\mathrm{res}} = \sum_{i=0}^{n} \left[1 - \frac{s_{\mathrm{model}}(\lambda_i)}{s_{\mathrm{meas}}(\lambda_i)} \right]^2 , \tag{3}$$

where the index $i = 0, 1, 2, ..., n$ runs over wavelengths, $s_{\mathrm{model}}(\lambda_i)$ is the spectral model and $s_{\mathrm{meas}}(\lambda_i)$ is the spectral measurement of a quantity to be fitted. Some instructions on carrying out the experimental measurements are discussed in Section 4.

Table 1: Free parameters to be fitted in the algorithm.

STEP 1:	Unit	*Spectral reflectance modelling from ultraviolet to near-infrared wavelengths*
$d_{\mathrm{SiO_2}}$	nm	Thickness of the silicon dioxide layer
STEP 2:		*Internal quantum efficiency at visible and near-infrared wavelengths*
P_{f}	–	Collection efficiency at the front surface
T	μm	Depth of unity collection efficiency
P_{r}	–	Bulk collection efficiency
D	μm	Depth for reaching P_{r}
d	μm	Thickness of the photodiode
STEP 3:		*Quantum yield at ultraviolet wavelengths*
B	1/m	Parameter to describe doping conditions
ΔE	eV	Shift in the photon energy scale due to the changing junction temperature

2.1 Spectral Reflectance

A silicon dioxide SiO_2 layer is naturally grown on the surface of a silicon photodiode and its thickness determines the reflectance from the photodiode. Snell's law and Fresnel equations are used for calculating the spectral reflectance of a trap detector. The trap detectors at the Metrology Research Institute consist of three silicon photodiode elements so that the incident angles of the first two reflections are 45º, third reflection angle is 0º, and the last two reflection angles are 45º. With this geometry, the two reflection planes are orthogonal [6],

5

and thus the total reflectance of the trap detector does not depend on the polarization of the incident light and it can be modelled with five reflections [7] as

$$\rho(\lambda) = \rho_{0^\circ}(\lambda) \cdot \rho_{s,45^\circ}(\lambda)^2 \cdot \rho_{p,45^\circ}(\lambda)^2 . \tag{4}$$

However, Goebel *et al.* [8, 9] have shown that even small misalignments from the ideal photodiode orientations and deviations in the SiO_2 layer thicknesses among the photodiodes would lead to the polarization dependence of a trap detector.

Figure 2 shows an example of fitting the spectral reflectance model in Eq. (4) to the reflectances measured for a trap detector at eight laser wavelengths, so that the thickness of a silicon dioxide layer is a free parameter.
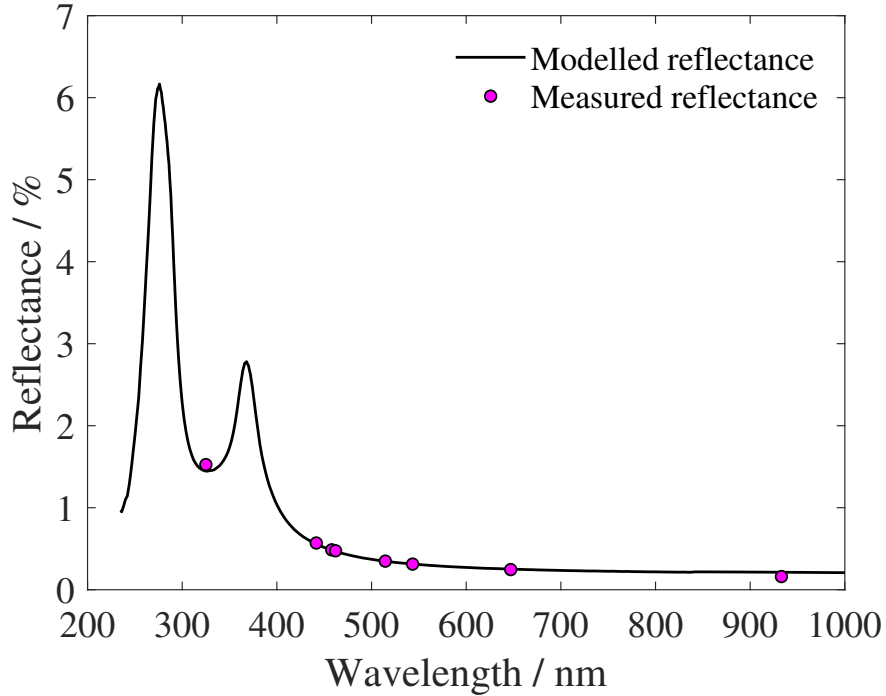
Figure 2: Spectral reflectance model fitted to the experimental reflectance data.

2.1.1 Spectral Reflectance at the Incident Angle of 0°

The total reflectance from the silicon photodiode at the incident angle of 0° is obtained as

$$\rho_{0^\circ}(\lambda) = \left| r_{12}(\lambda) + \frac{t_{12}(\lambda) \cdot t_{21}(\lambda) \cdot \bar{r}_{23}(\lambda) \cdot \exp\left[-2i \cdot \beta_{SiO_2,0^\circ}(\lambda)\right]}{1 + r_{12}(\lambda) \cdot \bar{r}_{23}(\lambda) \cdot \exp\left[-2i \cdot \beta_{SiO_2,0^\circ}(\lambda)\right]} \right|^2 \tag{5}$$

meaning that the total reflection consists of the direct reflection component $r_{12}(\lambda)$ followed by photon recycling due to finite transmissions and reflections on interfaces illustrated in Fig. 3 that forms a geometric series.

6

Figure 3: Reflectance from the layer structure of a silicon photodiode.

The phase term of the silicon dioxide layer is

$$\beta_{\mathrm{SiO_2},0^\circ}(\lambda) = \frac{2\pi}{\lambda} \cdot n_{\mathrm{SiO_2}}(\lambda)\, d_{\mathrm{SiO_2}}, \tag{6}$$

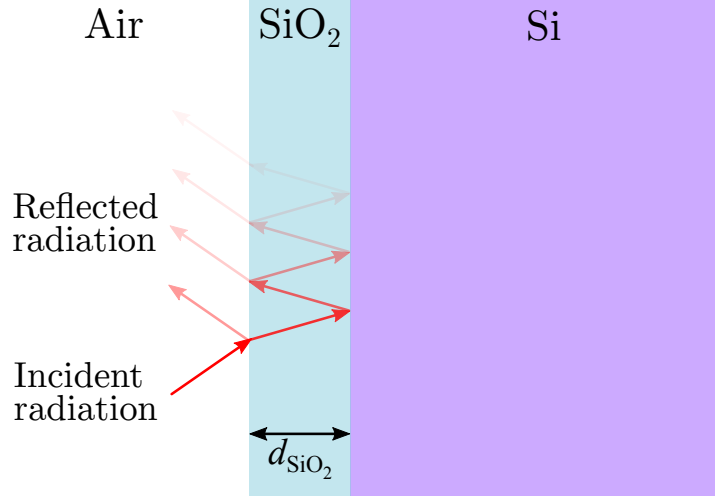where the $n_{\mathrm{SiO_2}}$ is the refractive index and $d_{\mathrm{SiO_2}}$ is the thickness of the silicon dioxide layer. The transmission and reflection scattering coefficients are defined as

$$t_{12}(\lambda) = \frac{2 \cdot n_{\mathrm{air}}(\lambda)}{n_{\mathrm{air}}(\lambda) + n_{\mathrm{SiO_2}}(\lambda)} \tag{7}$$

$$r_{12}(\lambda) = \frac{n_{\mathrm{SiO_2}}(\lambda) - n_{\mathrm{air}}(\lambda)}{n_{\mathrm{SiO_2}}(\lambda) + n_{\mathrm{air}}(\lambda)} \tag{8}$$

$$\bar{r}_{23}(\lambda) = \frac{\bar{n}_{\mathrm{Si}}(\lambda) - n_{\mathrm{SiO_2}}(\lambda)}{\bar{n}_{\mathrm{Si}}(\lambda) + n_{\mathrm{SiO_2}}(\lambda)} \tag{9}$$

$$t_{21}(\lambda) = \frac{2 \cdot n_{\mathrm{SiO_2}}(\lambda)}{n_{\mathrm{SiO_2}}(\lambda) + n_{\mathrm{air}}(\lambda)} \tag{10}$$

2.1.2 Spectral Reflectance for S-Polarized Light

The total reflectance of s-polarized light is

$$\rho_{\mathrm{s},45^\circ}(\lambda) = \left| r_{\mathrm{s},12}(\lambda) + \frac{t_{\mathrm{s},21}(\lambda) \cdot t_{\mathrm{s},12}(\lambda) \cdot \bar{r}_{\mathrm{s},23}(\lambda) \cdot \exp\left[-2i \cdot \beta_{\mathrm{SiO_2},45^\circ}(\lambda)\right]}{1 + r_{s,12}(\lambda) \cdot \bar{r}_{s,23}(\lambda) \cdot \exp\left[-2i \cdot \beta_{\mathrm{SiO_2},45^\circ}(\lambda)\right]} \right|^2 \tag{11}$$

where the phase factor is

$$\beta_{\mathrm{SiO_2},45^\circ}(\lambda) = \frac{2\pi}{\lambda} \cdot n_{\mathrm{SiO_2}} d_{\mathrm{SiO_2}} \cos\left[\theta_2(\lambda)\right] \tag{12}$$

and the transmission and reflection scattering coefficients are defined as

$$t_{\mathrm{s},12}(\lambda) = \frac{2 \cdot n_{\mathrm{air}}(\lambda) \cdot \cos\theta_1}{n_{\mathrm{air}}(\lambda) \cdot \cos\theta_1 + n_{\mathrm{SiO_2}}(\lambda) \cdot \cos\left[\theta_2(\lambda)\right]} \tag{13}$$

$$r_{\mathrm{s},12}(\lambda) = \frac{n_{\mathrm{air}}(\lambda) \cdot \cos\theta_1 - n_{\mathrm{SiO_2}}(\lambda) \cdot \cos\left[\theta_2(\lambda)\right]}{n_{\mathrm{air}}(\lambda) \cdot \cos\theta_1 + n_{\mathrm{SiO_2}}(\lambda) \cdot \cos\left[\theta_2(\lambda)\right]} \tag{14}$$

$$\bar{r}_{\mathrm{s},23}(\lambda) = \frac{\bar{n}_{\mathrm{SiO_2}}(\lambda) \cdot \cos\left[\theta_2(\lambda)\right] - n_{\mathrm{Si}}(\lambda) \cdot \cos\left[\theta_3(\lambda)\right]}{\bar{n}_{\mathrm{SiO_2}}(\lambda) \cdot \cos\left[\theta_2(\lambda)\right] + n_{\mathrm{Si}}(\lambda) \cdot \cos\left[\theta_3(\lambda)\right]} \tag{15}$$

$$t_{\mathrm{s},21}(\lambda) = \frac{2 \cdot n_{\mathrm{SiO_2}}(\lambda) \cdot \cos\left[\theta_2(\lambda)\right]}{n_{\mathrm{SiO_2}}(\lambda) \cdot \cos\left[\theta_2(\lambda)\right] + n_{\mathrm{air}}(\lambda) \cdot \cos\theta_1} \tag{16}$$

The refraction angles $\theta_2(\lambda)$ and $\theta_3(\lambda)$ in silicon dioxide and silicon can be calculated from Snell's law as

$$\theta_2(\lambda) = \arcsin\left(\frac{n_{\mathrm{air}}(\lambda) \cdot \sin\theta_1}{n_{\mathrm{SiO_2}}(\lambda)}\right) \tag{17}$$

$$\theta_3(\lambda) = \arcsin\left(\frac{n_{\mathrm{SiO_2}}(\lambda) \cdot \sin\left[\theta_2(\lambda)\right]}{n_{\mathrm{Si}}(\lambda)}\right) \tag{18}$$

with the incident angle $\theta_1 = \pi/4$.

2.1.3   Spectral Reflectance for P-Polarized Light

The total reflectance of p-polarized light is

$$\rho_{\mathrm{p},45°}(\lambda) = \left| r_{\mathrm{p},12}(\lambda) + \frac{t_{\mathrm{p},12}(\lambda) \cdot t_{\mathrm{p},21}(\lambda) \cdot \bar{r}_{\mathrm{p},23}(\lambda) \cdot \exp\left[-2i \cdot \beta_{\mathrm{SiO_2},45°}(\lambda)\right]}{1 + r_{\mathrm{p},12}(\lambda) \cdot \bar{r}_{\mathrm{p},23}(\lambda) \cdot \exp\left[-2i \cdot \beta_{\mathrm{SiO_2},45°}(\lambda)\right]} \right|^2, \tag{19}$$

where the transmission and reflection scattering coefficients are defined as

$$t_{\mathrm{p},12}(\lambda) = \frac{2 \cdot n_{\mathrm{air}}(\lambda) \cdot \cos\theta_1}{n_{\mathrm{SiO_2}}(\lambda) \cdot \cos\theta_1 + n_{\mathrm{air}}(\lambda) \cdot \cos\left[\theta_2(\lambda)\right]} \tag{20}$$

$$r_{\mathrm{p},12}(\lambda) = \frac{n_{\mathrm{SiO_2}}(\lambda) \cdot \cos\theta_1 - n_{\mathrm{air}}(\lambda) \cdot \cos\left[\theta_2(\lambda)\right]}{n_{\mathrm{SiO_2}}(\lambda) \cdot \cos\theta_1 + n_{\mathrm{air}}(\lambda) \cdot \cos\left[\theta_2(\lambda)\right]} \tag{21}$$

$$\bar{r}_{\mathrm{p},23}(\lambda) = \frac{\bar{n}_{\mathrm{Si}}(\lambda) \cdot \cos\left[\theta_2(\lambda)\right] - n_{\mathrm{SiO_2}}(\lambda) \cdot \cos\left[\theta_3(\lambda)\right]}{\bar{n}_{\mathrm{Si}}(\lambda) \cdot \cos\left[\theta_2(\lambda)\right] + n_{\mathrm{SiO_2}}(\lambda) \cdot \cos\left[\theta_3(\lambda)\right]} \tag{22}$$

$$t_{\mathrm{p},21}(\lambda) = \frac{2 \cdot n_{\mathrm{SiO_2}}(\lambda) \cdot \cos\left[\theta_2(\lambda)\right]}{n_{\mathrm{SiO_2}}(\lambda) \cdot \cos\left[\theta_2(\lambda)\right] + n_{\mathrm{air}}(\lambda) \cdot \cos\theta_1} \tag{23}$$

2.1.4   Refractive Indices

Metals and semiconductors have a complex refractive index defined as [7]

$$\bar{n}(\lambda) = n(\lambda) - i\kappa(\lambda), \tag{24}$$

where $n(\lambda)$ is the real part and $\kappa(\lambda)$ is the imaginary part. The imaginary part attenuates the transmitting radiation in medium and it corresponds to the absorption coefficient (μm^{-1}) with a following relationship:

$$\alpha(\lambda) = \frac{4\pi}{\lambda} \kappa(\lambda). \tag{25}$$

A refractive index depends on the temperature of a medium. The measurements needed for modelling the spectral responsivity of trap detectors are usually performed in the typical room temperature conditions. The literature values from [10] were earlier used for the complex refractive index of a silicon (Si) at typical room temperature. In the latest version of the model, the temperature dependent refractive index of a silicon is taken into account with the model by Green [11] as

$$n_{\text{Si},T}(\lambda) = n_{\text{Si},300\,\text{K}}(\lambda) \cdot \left(\frac{T}{300\,\text{K}}\right)^{C_n(\lambda)\cdot 300\,\text{K}}, \tag{26}$$

$$\kappa_{\text{Si},T}(\lambda) = \kappa_{\text{Si},300\,\text{K}}(\lambda) \cdot \left(\frac{T}{300\,\text{K}}\right)^{C_\kappa(\lambda)\cdot 300\,\text{K}}, \tag{27}$$

where $C_n(\lambda)$ and $C_\kappa(\lambda)$ are temperature coefficients given in $10^{-4}\,\text{K}^{-1}$.

Dielectric media do not attenuate the transmitting radiation and their refractive index is a real number. For example, the refractive index of a silicon dioxide (SiO_2) at room temperature is obtained with Sellmeir's equation [12, 13] as

$$n_{\text{SiO}_2} = \sqrt{\frac{0.6961663 \cdot \lambda^2}{\lambda^2 - 0.0684043^2} + \frac{0.4079426 \cdot \lambda^2}{\lambda^2 - 0.1162414^2} + \frac{0.8974794 \cdot \lambda^2}{\lambda^2 - 9.896161^2} + 1}, \tag{28}$$

where λ is the radiation wavelength in μm. The refractive index of air at room temperature is obtained [14] as

$$n_{\text{air}} = \frac{0.05792105}{238.0185 - \lambda^{-2}} + \frac{0.00167917}{57.362 - \lambda^{-2}} + 1. \tag{29}$$

The refractive index dependence with changing temperature were not taken into account for SiO_2 and air. Changes in SiO_2 temperature would slightly alter the modelled thickness of the SiO_2 layer.

2.2 Internal Quantum Efficiency

The internal quantum efficiency in the visible and near-infrared wavelength region is defined [4] as

$$\epsilon_i(\lambda) = \int_0^d \alpha(\lambda)\, P(x) \cdot \exp\left[-\alpha(\lambda)\, x\right] \mathrm{d}x, \tag{30}$$

when the absorption coefficient $\alpha(\lambda)$ and the collection efficiency $P(x)$ are known. This integral can be calculated by a piecewise summation of the local collection efficiencies over the regions presented in Fig. 4. The internal quantum efficiency can be derived from the

geometrical presentation of Fig. 4 according to Gentile *et al.* [4] and Werner *et al.* [15] as

$$
\begin{aligned}
\epsilon_i(\lambda) = P_{\mathrm{f}} &+ \frac{1 - P_{\mathrm{f}}}{\alpha(\lambda)\,T} \cdot \{1 - \exp\left[-\alpha(\lambda)\,T\right]\} \\
&- \frac{1 - P_{\mathrm{r}}}{\alpha(\lambda)\,[D - T]} \cdot \{\exp\left[-\alpha(\lambda)\,T\right] - \exp\left[-\alpha(\lambda)\,D\right]\} \\
&- P_{\mathrm{r}} \cdot \exp\left[-\alpha(\lambda)\,d\right] + \rho_{\mathrm{r}} P_{\mathrm{r}} \cdot \exp\left[-\alpha(\lambda)\,d\right],
\end{aligned}
\tag{31}
$$

where $\alpha(\lambda)$ is the absorption coefficient at room temperature, P_{f} is the collection efficiency at the $\mathrm{SiO_2/Si}$ interface, T is the depth in the photodiode at which the collection efficiency is unity, P_{r} is the collection efficiency in the rear region of the photodiode, D is the depth at which the collection efficiency has linearly decreased to the value of P_{r}, d is the thickness of the photodiode, and ρ_{r} is the reflection coefficient of the rear surface. The back reflection effect $\rho_{\mathrm{r}} P_{\mathrm{r}} \cdot \exp\left[-\alpha(\lambda)\,d\right]$ in Eq. (31) is neglected in the spectral model to reduce the number of free fitting parameters.
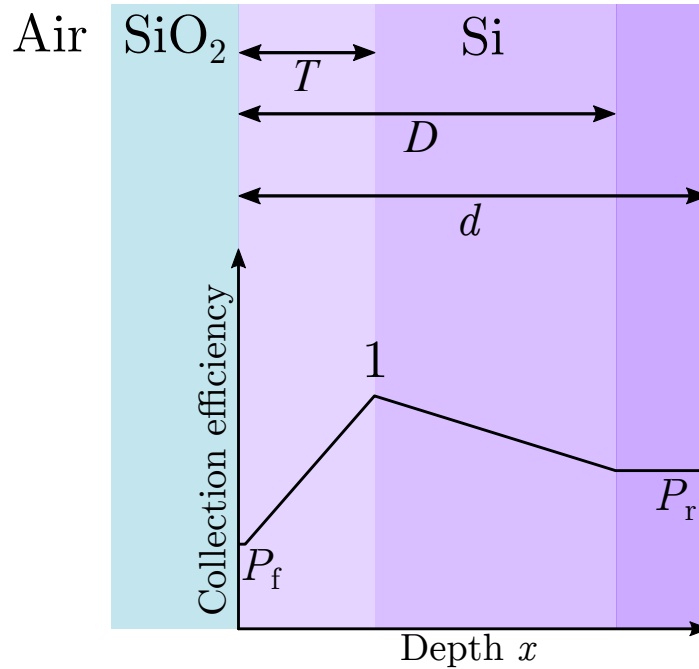
Figure 4: Layer structure of a silicon photodiode and the collection efficiency as a function of the penetration depth of photons.

2.3 Quantum Yield in the Ultraviolet Wavelength Region

In the ultraviolet wavelength region, one incident energetic photon can produce more than one electron-hole pair in silicon, meaning that the quantum yield exceeds unity. The quantum yield at the photon energy scale is defined as

$$
\eta(\hbar\omega) = 1 + \int P(\hbar\omega, E) \cdot N(E)\,\mathrm{d}E,
\tag{32}
$$

10

where unity describes one electron-hole pair created by the original absorption process, $N(E)$ represents the effect of electron-phonon scattering on the average number of electron-hole pairs, and $P(\hbar\omega, E)$ is the probability of electron excitation after photon absorption.

The general relationship between the absorption coefficient (μm^{-1}) and the density of states ($cm^{-3}eV^{-1}$) is defined as

$$\alpha(E) \propto g_c(E_c) \cdot P(E) \cdot g_v(E_v), \tag{33}$$

where E depicts the energy scale. As most of the impact ionization occur from valence band top to deep in the conduction band [16], the density of states in the valence band $g_v(E_v)$ can be neglected and the probability of electron excitation to the conduction band after photon absorption becomes

$$P(\hbar\omega) \approx Ba^3 \cdot \frac{g_c(\hbar\omega)}{\alpha(\hbar\omega)}, \tag{34}$$

where $\alpha(\hbar\omega)$ (μm^{-1}) is the absorption coefficient and $g_c(\hbar\omega)$ ($cm^{-3}eV^{-1}$) is the density of states in the conduction band at photon energy $\hbar\omega = E - \Delta E$. The density of states and the absorption coefficient are functions of the junction temperature, the junction temperature dependence is taken into account with the energy shift ΔE (eV). A scaling factor B (μm^{-1}) includes the transition-matrix element, $a = 0.5431$ nm is the lattice constant of silicon at room temperature [17].

The electron-phonon scattering probability $N(\hbar\omega - E_g^X)$ of the impact ionized electrons is defined by Alig *et al.* [18] as

$$N(\hbar\omega - E_g^X) = \left[1 + \frac{105A}{2\pi} \cdot \frac{(\hbar\omega - E_g^X - \hbar\omega_{ph})^{1/2}}{(\hbar\omega - 2E_g^X)^{7/2}}\right]^{-1}, \tag{35}$$

where $\hbar\omega_{ph} = 62$ meV is the energy of optical phonon in silicon, the constant A is set to 5.2 eV^3, $E_g^X = 1.12$ eV is the indirect band gap at X point of the reciprocal lattice of silicon, and $2E_g^X$ is the theoretical threshold energy for impact ionization.

With these definitions and approximation of the integral, Eq. (32) becomes

$$\eta(\lambda) = 1 + Ba^3 \cdot \frac{g_c(\hbar\omega)}{\alpha(\hbar\omega)} \cdot N(\hbar\omega - E_g^X) \cdot (\hbar\omega - E_g^\Gamma), \tag{36}$$

where $E_g^\Gamma = 3.1$ eV is the direct excitation at the Γ point of the reciprocal lattice of silicon. The spectral quantum yield model of Eq. (36) is fitted to the experimental quantum yield in Figs. 5 and 6.
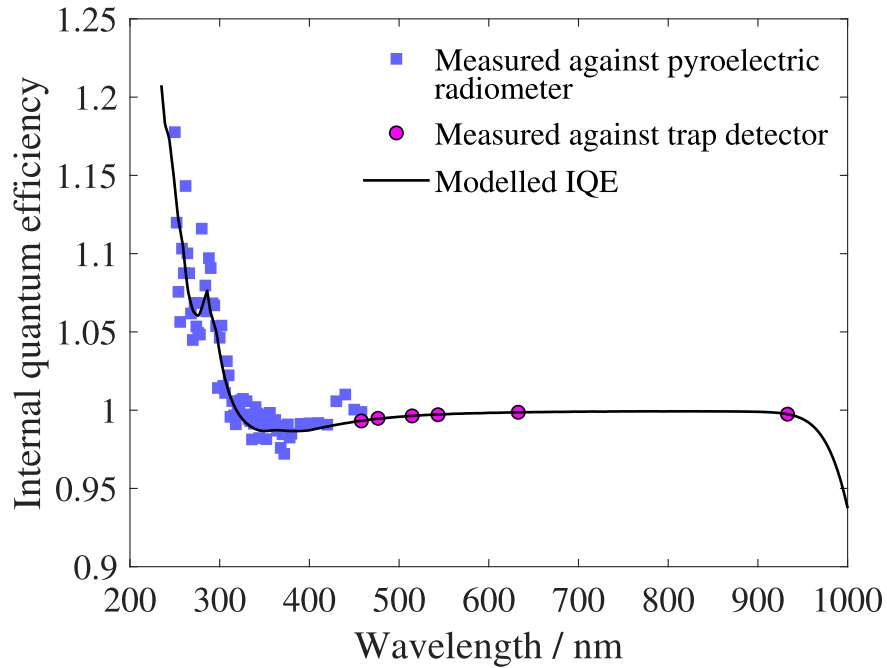
Figure 5: Spectral internal quantum efficiency model of a trap detector with quantum yield taken into account.
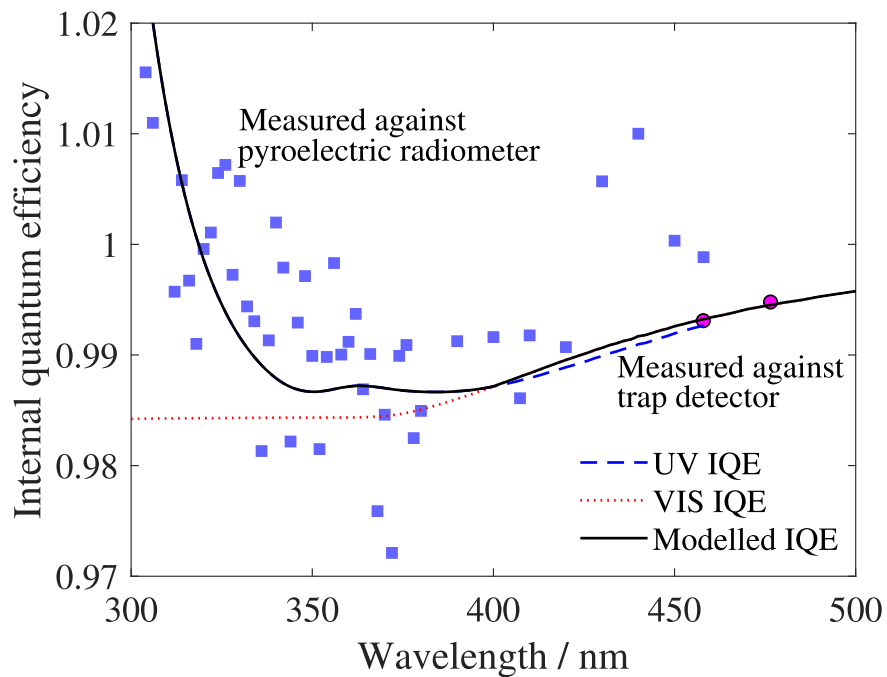

Figure 6: Zoomed internal quantum efficiency model of a trap detector.

12

2.3.1 Density of States

The density of states in the conduction band can be calculated from the energy band gradients as [19]

$$g_c(\hbar\omega) = \frac{2}{8\pi^3} \int\int \frac{1}{|\nabla_k(E_c)|} dS, \tag{37}$$

where k is the wave vector and E_c is the energy scale of the conduction band. The gradient for 3D structure can be determined as

$$|\nabla_k(E_c)| = \sqrt{\left(\frac{\partial E_c}{\partial k_x}\right)^2 + \left(\frac{\partial E_c}{\partial k_y}\right)^2 + \left(\frac{\partial E_c}{\partial k_z}\right)^2}. \tag{38}$$

Figure 7 shows the 3D density of states in the conduction band of silicon as cross symbols. The effective DOS plotted as (solid and dashed curves) is obtained by fitting an exponential function to the low-energy slope of the DOS peak at 4.1 eV as experimental semiconductor spectra have exponential tails [20].
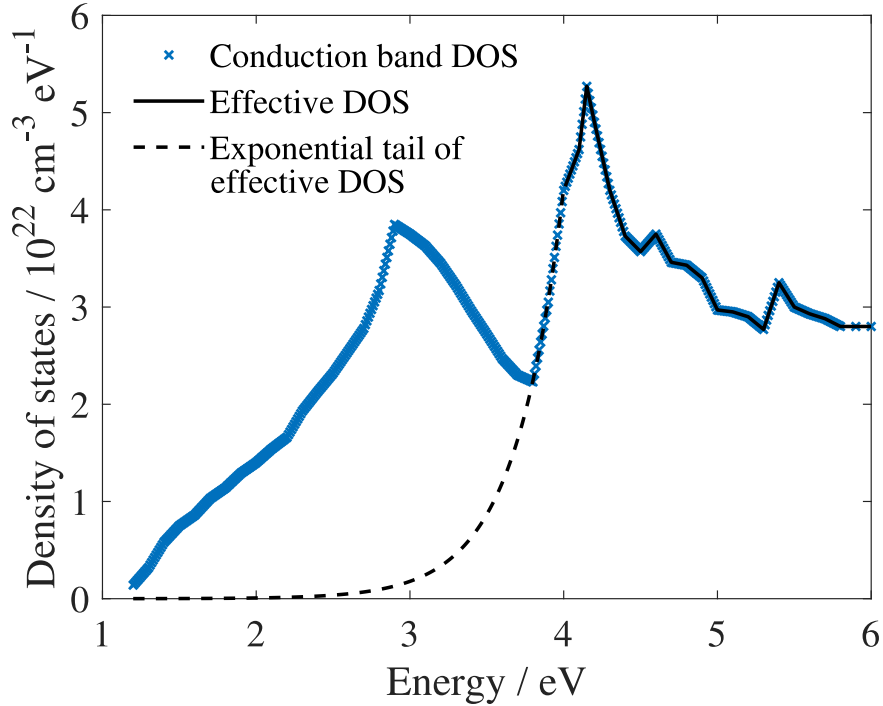

Figure 7: 3D density of states in the conduction band (cross symbols) and the corresponding effective DOS (solid and dashed curves).

3 Modelling Program

3.1 Use of the Program

The measurement program consists of one Matlab script *program_for_modelling_trap_responsivities_main_V1.m* with the following functions:

- Function *fit_spectral_reflectance*

- Function *fit_internal_quantum_efficiency*

- Function *fit_quantum_yield*

The measurements needed prior modelling are included in the input Excel file *template_trap_ID.xlsx* described in Chapter 3.2, which should be re-labelled for appropriately and placed in the same folder with the Matlab script. Please, make sure that the Excel file intended to import by Matlab script matches with the re-labelled name. Matlab script of the program including the fitting functions are given in Chapter 3.3.

3.2 Input Excel File

An Excel file with three spreadsheets introduced in Table 2 is used for importing and exporting data. The data sets in the spreadsheets 'Measurement' and 'n(Si)' are imported and used by the Matlab script. The modelling results are saved in the spreadsheet 'Model'.

Table 2: Free parameters to be fitted in the algorithm.

Spreadsheet: Measurements

Column A	Wavelength (nm)
Column B	Reflectance (unitless)
Column C	Relative standard uncertainty (unitless)
Column F	Wavelength (nm)
Column G	Responsivity measured at VIS (A/W)
Column J	Wavelength (nm)
Column K	Responsivity measured at UV (A/W)

Spreadsheet: n(Si)

Column A	Wavelength (nm)
Column B	Real part of the refractive index n(Si) at 300 K
Column C	Imaginary part of the refractive index κ(Si) at 300 K
Column D	Temperature coefficient C_n(Si) for the real part of the refractive index n(Si)
Column E	Temperature coefficient C_κ(Si) for the imaginary part of the refractive index κ(Si)
Column I	Energy (eV)
Column J	Density of states in the conduction band
Column K	Density of states in the valence band

Spreadsheet: Model

Column A	Wavelength (nm)
Column B	Reflectance (unitless)
Column C	IQE (unitless)
Column D	Ideal responsivity (A/W)
Column E	Modelled responsivity (A/W)
Cell K1	d_{SiO_2} = Thickness of SiO_2 (nm)
Cell K2	P_f = Collection efficiency at front surface
Cell K3	T = Depth of unity collection efficiency (um)
Cell K4	P_r = Bulk collection efficiency
Cell K5	D = Depth for reaching P_r (um)
Cell K6	d = Thickness of diode (um)
Cell K7	B = Scaling factor (1/m)
Cell K8	ΔE = Energy shift (eV)

3.3 Matlab Script

The Matlab program contains one Matlab script labelled as *program_for_modelling_trap_responsivities_main_V1.m* that includes all the functions.

Listing 1: Script for modelling the spectral reflectance of a trap detector.

```matlab
% ----- Main program for trap detector v. 1.0 -----
%
%
% Reference:
%      A. Vaskuri and P. Karha, "Instruction Manual for the Spectral
%      Modelling of Silicon Trap Detectors," Metrology Research Institute,
%      Version 1.0 (2019).
%
% -----

% Clear Matlab parameters
clear all; close all; clc;

% Set font and fontsize
set(0, 'DefaultTextFontname', 'Times New Roman', ...
    'DefaultAxesFontsize', 16, 'DefaultTextFontsize', 16);
set(0, 'DefaultAxesFontName', 'Times New Roman', ...
    'DefaultAxesFontsize', 16, 'DefaultTextFontsize', 16);

% ----- Import measurement data, insert values here -----
% File name for trap detector
name = 'template_trap_ID';

% Folder where measurement file is located
folder = '\';

% Complete path for the measurement file
file = strcat(folder, name, '.xlsx');

% Set temperature / K (Default 296 K)
temperature = 296;

% Import complex refractive index
% Column A: Wavelengths / nm
% Column B: n(Si) at 300 K
% Column C: k(Si) at 300 K
% Column D: Cn(Si)
% Column E: Ck(Si)
M_refractive_index = xlsread(file, 'n(Si)', 'A2:E2402');
wl_n_Si = M_refractive_index(:, 1);
n_Si_300K = M_refractive_index(:, 2);
k_Si_300K = M_refractive_index(:, 3);
Cn_Si = M_refractive_index(:, 4);
Ck_Si = M_refractive_index(:, 5);

% Temperature dependence of the refractive index of a silicon, Eqs. (26-27)
```

```matlab
47  n_Si_real = n_Si_300K.*((temperature./300).^((Cn_Si.*300)./10000));
48  k_Si_imaginary = k_Si_300K.*((temperature./300).^((Ck_Si.*300)./10000));
49
50  % Import electron density of states
51  % Column E: Energies / eV
52  % Column F: Conduction band DOS / 10^22 /(eV * cm^3)
53  % Column G: Valence band DOS / 10^22 /(eV * cm^3)
54  M_DensityOfStates = xlsread(file, 'n(Si)', 'G2:I464');
55  E_DOS = M_DensityOfStates(:, 1);
56  DOS_electrons = M_DensityOfStates(:, 2);
57
58  % Import measured reflectances with the relative uncertainties (k = 2)
59  % Column A: Wavelengths / nm
60  % Column B: Reflectances measured / dimensionless
61  % Column C: Relative standard uncertainty / dimensionless
62  M_refl = xlsread(file, 'Measurements', 'A2:C50');
63  wl_meas_refl = M_refl(:, 1);
64  reflectance_measured = M_refl(:, 2);
65  uncertainty_reflectance = M_refl(:, 3);
66
67  % Import responsivities (A/W) measured with the trap detector
68  % Column F: Wavelengths / nm
69  % Column G: Responsivities / A/W
70  M_trap_resp = xlsread(file, 'Measurements', 'F2:G50');
71  responsivity = M_trap_resp(1:end, 2);
72  wl_meas_nm = M_trap_resp(1:end, 1);
73
74  % Import responsivities (A/W) measured in the ultraviolet wavelength
75  % region with the pyroelectric radiometer
76  % Column J: Wavelengths / nm
77  % Column K: Responsivities / A/W
78  M_pyro_resp = xlsread(file, 'Measurements', 'J2:K100');
79  % -----
80
81  % ----- Spectral ranges -----
82  % Step size of the modelled results / nm
83  dist = 1;
84  % Define wavelength ranges for visible (VIS) and ultraviolet (UV)
85  uvEnd = M_pyro_resp(end, 1);              % End of the UV range
86  uvStart = 235;                           % Begin of the UV range
87  visStart = 235;                          % Begin of the visible range
88  visEnd = 1000;                           % End of the visible range
89  VIS_wl_nm = [visStart:dist:visEnd]';
90  UV_wl_nm = [uvStart:dist:uvEnd]';
91  wl_nm = [uvStart:dist:visEnd]';          % Full wavelength scale
92  % UV and visible models are combined at 400 nm
93  wl_change_model_from_UV_to_VIS = 400;
94  % -----
95
96  % ----- Complex refractive index, Eq. (24) -----
97  n_Si_temp = n_Si_real - 1i*k_Si_imaginary;
98  % Interpolate to match with the wavelength scale
99  n_Si = interp1(wl_n_Si, n_Si_temp, wl_nm);
100 % -----
```

```matlab
101
102 % ----- Absorption coefficient of silicon, Eq. (25) -----
103 alpha_temp = (4*pi*k_Si_imaginary)./(wl_n_Si*1e-3);
104 % Interpolate to match with the wavelength scale
105 alpha = interp1(wl_n_Si, alpha_temp, wl_nm);
106 % -----
107
108 % ----- Nature constants -----
109 global h_eV c
110 e = 1.6021892e-19;                      % Elementary charge / C
111 h_J = 6.62608e-34;                      % Planck constant / J*s
112 h_eV = 4.13566766225*1e-15;             % Planck constant / eV*s
113 c = 2.99792458*1e8;                     % Speed of light in vacuum / m/s
114 % -----
115
116 % ----- Spectral reflectance of a trap detector -----
117 [thickness, modelled_reflectance] = reflectanceModel(wl_meas_refl, ...
118     reflectance_measured, wl_nm, n_Si);
119 [thicknessMin, modelled_reflectance_min] = reflectanceModel(wl_meas_refl, ...
120     reflectance_measured.*(1 - uncertainty_reflectance), wl_nm, n_Si);
121 [thicknessMax, modelled_reflectance_max] = reflectanceModel(wl_meas_refl, ...
122     reflectance_measured.*(1 + uncertainty_reflectance), wl_nm, n_Si);
123 disp('STEP 1: Modelled spectral reflectance ready.');
124 % -----
125
126 % ----- Fit internal quantum efficiency in the visible spectral region -----
127 wl_meas_um = wl_meas_nm/1000;
128 responsivity_ideal = (e*wl_meas_um)/(h_J*c)/1e6;
129 reflectance_meas = interp1(wl_nm, modelled_reflectance, wl_meas_nm);
130 alpha_um = interp1(wl_nm, alpha, wl_meas_nm);
131 internal_quantum_efficiency_ref = responsivity./(1 - reflectance_meas) ...
132     ./responsivity_ideal;
133
134 x0 = [0.95 0.3 0.995 20 300]; % Initial guess values
135 lb = [0 0 0 0 0];     % Lower limits
136 ub = [1 Inf 1 Inf Inf];       % Upper limits
137 options = optimoptions(@lsqnonlin, 'Algorithm', 'trust-region-reflective', ...
138     'MaxFunEvals', 10000, 'MaxIter', 10000, 'StepTolerance', 1e-10, ...
139     'OptimalityTolerance', 1e-10, 'FunctionTolerance', 1e-10, ...
140     'Display', 'off');
141 x = lsqnonlin(@(x) fit_internal_quantum_efficiency(x, alpha_um, ...
142     internal_quantum_efficiency_ref), x0, lb, ub, options);
143 Pf = x(1);            % Collection efficiency at front surface
144 T = x(2);             % Depth of unity collection efficiency / um
145 Pr = x(3);            % Bulk collection efficiency
146 D = x(4);             % Depth for reaching efficiency Pr / um
147 ThD = x(5);           % Thickness of the photodiode / um
148
149 modelled_reflectance_VIS = interp1(wl_nm, modelled_reflectance, VIS_wl_nm);
150 alpha_VIS = interp1(wl_nm, alpha, VIS_wl_nm);
151
152 % Optimized internal quantum efficiency at visible region, Eq. (31)
153 IQE_VIS = Pf + (1 - Pf)./(alpha_VIS.*T).*(1 - exp(-alpha_VIS.*T)) ...
154     - (1 - Pr)./alpha_VIS/(D - T).*(exp(-alpha_VIS.*T) ...
```

```matlab
155         - exp(-alpha_VIS.*D)) - Pr.*exp(-alpha_VIS.*ThD);
156
157     responsivity_ideal_VIS = (e*VIS_wl_nm/1000)/(h_J*c)/1e6;
158
159     % Modelled trap responsivity Eq. (1)
160     responsivity_model_VIS = (1 - modelled_reflectance_VIS).*IQE_VIS ...
161         .*responsivity_ideal_VIS;
162     responsivity_ideal_model = (e*wl_nm/1000)/(h_J*c)/1e6;
163
164     disp('STEP 2: Modelled IQE in the visible region ready.');
165     % -----
166
167     % ----- Fit quantum yield in the ultraviolet spectral region -----
168     wl_pyro_meas = M_pyro_resp(:, 1);
169     responsivity_pyro_meas = M_pyro_resp(:, 2);
170
171     ideal_responsivity_pyro_UV = (e*wl_pyro_meas/1000)/(h_J*c)/1e6;
172     modelled_reflectance_pyro_UV = interp1(wl_nm, modelled_reflectance, wl_pyro_meas);
173     alpha_UV = interp1(wl_nm, alpha, wl_pyro_meas);
174
175     % Internal quantum efficiency at visible region Eq. (4)
176     IQE_UV = Pf + (1 - Pf)./(alpha_UV.*T).*(1 - exp(-alpha_UV.*T)) ...
177         - (1 - Pr)./alpha_UV./(D - T).*(exp(-alpha_UV.*T) - exp(-alpha_UV.*D)) ...
178         - Pr.*exp(-alpha_UV.*ThD);
179
180     % Measured IQE, uvRtrap depicts the reflectance
181     quantum_yield_pyro_meas = responsivity_pyro_meas ...
182     ./ideal_responsivity_pyro_UV./(1 - modelled_reflectance_pyro_UV)./IQE_UV;
183
184     % ----- Fit quantum yield at UV region -----
185     x0 = [1 0];          % Initial guess values
186     lb = [0 -0.5];       % Lower limits
187     ub = [1e8 0.5];      % Upper limits
188     options = optimoptions(@lsqnonlin, 'Algorithm', 'trust-region-reflective', ...
189         'MaxFunEvals', 10000, 'MaxIter', 10000, 'StepTolerance', 1e-10, ...
190         'OptimalityTolerance', 1e-10, 'FunctionTolerance', 1e-10, ...
191         'Display', 'off');
192     x = lsqnonlin(@(x) fit_quantum_yield(x, wl_pyro_meas, ...
193         quantum_yield_pyro_meas, E_DOS, DOS_electrons, alpha_UV), x0, ...
194         lb, ub, options);
195     B = x(1);
196     deltaE = x(2);
197
198     E = (h_eV.*c)./(UV_wl_nm*1e-9);
199     hw = E - deltaE;
200
201     a = 0.543;           % Lattice constant of Si / nm
202     A = 5.2;             % Empirical constant / eV^3
203     hw0 = 0.062;         % Phonon energy / eV
204     Eg_in = 1.12;        % Indirect transition / eV
205     Eg_d = 3.1;          % Direct transition / eV
206
207     % Electron density of states
208     E_DOS_slope = E_DOS(find(E_DOS >= 3.8 & E_DOS <= 4.0));
```

```matlab
209  DOS_UV_slope =  DOS_electrons(find(E_DOS >= 3.8 & E_DOS <= 4.0));
210
211  params = polyfit(E_DOS_slope, log(DOS_UV_slope), 1);
212  tail_fit = exp(polyval(params, E_DOS(find(E_DOS <= 4.0))));
213
214  % Effective electron density of states
215  DOS_UV_temp = [tail_fit; DOS_electrons(find(E_DOS > 4.0))];
216  DOS_UV = 10*interp1(E_DOS - deltaE, DOS_UV_temp, E, 'pchip');
217
218  alpha_UV = interp1(wl_nm, alpha, UV_wl_nm);
219  % Spectral internal quantum efficiency in the visible and
220  % near-infrared regions
221  IQE_UV = Pf + (1 - Pf)./(alpha_UV.*T).*(1 - exp(-alpha_UV.*T)) ...
222      - (1 - Pr)./alpha_UV./(D - T).*(exp(-alpha_UV.*T) - exp(-alpha_UV.*D)) ...
223      - Pr.*exp(-alpha_UV.*ThD);
224
225  E_alpha = (h_eV.*c)./(wl_nm*1e-9);
226  alpha_UV = interp1(E_alpha - deltaE, alpha, E);
227
228  % Modelled quantum yield
229  modelled_QY = 1 + ((a^3*B).*(DOS_UV./alpha_UV)./(1 + 105*A./(2*pi) ...
230      .*((hw - Eg_in - hw0).^(1/2))./((hw - 2*Eg_in).^(7/2))).*(E - Eg_d));
231
232  ideal_responsivity_UV = (e*UV_wl_nm/1000)/(h_J*c)/1e6;
233  modelled_reflectance_UV = pchip(wl_nm, modelled_reflectance, UV_wl_nm);
234
235  responsivity_model_UV = (1 - modelled_reflectance_UV).*IQE_UV ...
236      .*modelled_QY.*ideal_responsivity_UV;
237
238  IQE_pyro = M_pyro_resp(:, 2)./pchip(wl_meas_nm, responsivity_ideal, ...
239      M_pyro_resp(:, 1))./(1 - pchip(wl_nm, modelled_reflectance, ...
240      M_pyro_resp(:, 1)));
241  disp('STEP 3: Modelled quantum yield in the ultraviolet region ready.');
242  % -----
243
244  % ----- Combine UV and VIS models -----
245  idx_UV = find(UV_wl_nm >= wl_change_model_from_UV_to_VIS, 1);
246  idx_VIS = find(VIS_wl_nm >= wl_change_model_from_UV_to_VIS, 1);
247  responsivity_model = [responsivity_model_UV(1:idx_UV - 1); ...
248      responsivity_model_VIS(idx_VIS:end)];
249  IQE = [IQE_UV(1:idx_UV - 1).*modelled_QY(1:idx_UV - 1); ...
250      IQE_VIS(idx_VIS:end)];
251  % -----
252
253  % ----- Save the model and with the corresponding parameters -----
254  name = [name '_' datestr(now,'dd_mm_yyyy')];
255  xlswrite(file, {'Trap detector:', name}, 'Model', 'A1');
256  % Save the modelled reflectance, the internal quantum efficiency,
257  % ideal spectral responsivity, and modelled spectral responsivity
258  xlswrite(file, {'Wavelength [nm]', 'Reflectance', 'IQE', ...
259      'Ideal responsivity', 'Modelled responsivity'}, 'Model', 'A3');
260  xlswrite(file, [wl_nm modelled_reflectance IQE responsivity_ideal_model ...
261      responsivity_model], 'Model', 'A4');
262  % Save the optimized parameters
```

```
263  xlswrite(file, {'Thickness of SiO2 (nm)', ...
264      thickness; 'Collection efficiency at front surface', ...
265      Pf; 'Depth of unity collection efficiency (um)', ...
266      T; 'Bulk collection efficiency', Pr; 'Depth for reaching Pr (um)', ...
267      D; 'Thickness of the photodiode (um)', ...
268      ThD; 'Scaling factor (1/m)', B, 'Energy shift (eV)', deltaE}, ...
269      'Model', 'J1');
270  % Close the Excel file
271  fclose('all');
272  disp('Program ready.');
273  % -----
```

Listing 2: Script for plotting the modelling results.

```
1   % ----- Plot modelling results -----
2   % Plot spectral reflectance
3   figure;
4   set(gcf, 'color', 'w');
5   plot(wl_nm, 100*modelled_reflectance, 'k', 'linewidth', 1.2);
6   hold on;
7   plot(wl_meas_refl, 100*reflectance_measured, 'mo', 'MarkerFace', 'm', ...
8       'MarkerEdge', 'k', 'MarkerSize', 5);
9   hold off;
10  xlabel('Wavelength / nm');
11  ylabel('Reflectance / %');
12  set(gca, 'xtick', 0:100:2000);
13  legend('Modelled reflectance', 'Measured reflectance');
14  legend('boxoff');
15
16  % Plot spectral responsivity
17  figure;
18  set(gcf, 'color', 'w');
19  plot(M_pyro_resp(:, 1), M_pyro_resp(:, 2), 's', ...
20      'MarkerFace', [0.4, 0.4, 1], 'MarkerEdge', [0.4, 0.4, 1], ...
21      'MarkerSize', 6);
22  hold on;
23  plot(wl_meas_nm, responsivity, 'o', 'MarkerFace', 'm', ...
24      'MarkerEdge', 'k', 'MarkerSize', 6);
25  plot(wl_nm, responsivity_model, 'k', 'linewidth', 1.2);
26  set(gca, 'xtick', 0:100:2000);
27  xlabel('Wavelength / nm');
28  ylabel('Responsivity / A/W');
29  legend('Measured against pyroelectric radiometer', ...
30      'Measured against trap detector', 'Modelled responsivity', ...
31      'Location', 'NorthWest');
32  legend('boxoff');
33
34  % Plot spectral responsivity in the UV region
35  figure;
36  set(gcf, 'color', 'w');
37  plot(M_pyro_resp(:, 1), M_pyro_resp(:, 2), 's', 'MarkerFace', [0.4, 0.4, 1], 'MarkerEdge',
38  hold on;
39  plot(UV_wl_nm, responsivity_model_UV, 'k', 'linewidth', 1.2);
```

```matlab
40  hold off;
41  xlim([230 480]);
42  xlabel('Wavelength / nm');
43  ylabel('Responsivity / A/W');
44
45  % Plot spectral residual in the UV region
46  figure;
47  set(gcf, 'color', 'w');
48  plot(wl_pyro_meas, 100*(1 - spline(UV_wl_nm, modelled_QY, ...
49      wl_pyro_meas)./quantum_yield_pyro_meas), 'x-', 'linewidth', 1.2);
50  xlim([230 480]);
51  xlabel('Wavelength / nm');
52  ylabel('Residual / %');
53
54  % Plot density of states
55  figure;
56  set(gcf, 'color', 'w');
57  plot(E_DOS, DOS_electrons, 'x', 'markersize', 5, 'linewidth', 1.2);
58  hold on;
59  plot(E_DOS(find(E_DOS > 4.0)), DOS_electrons(find(E_DOS > 4.0)), ...
60      'k-', 'linewidth', 1.5);
61  plot(E_DOS(find(E_DOS <= 4.0)), tail_fit, 'k--', 'linewidth', 1.5);
62  hold off;
63  xlabel('Energy / eV');
64  ylabel('Density of states / 10^{22} cm^{-3} eV^{-1}');
65  legend('Conduction band DOS', 'Effective DOS', ...
66      'Exponential tail of effective DOS', 'location', 'northwest');
67  legend('boxoff');
68
69  % Plot internal quantum efficiency
70  figure;
71  set(gcf, 'color', 'w');
72  plot(M_pyro_resp(:, 1), IQE_pyro, 's', 'MarkerFace', [0.4, 0.4, 1], ...
73      'MarkerEdge', [0.4, 0.4, 1], 'MarkerSize', 6);
74  hold on;
75  plot(wl_meas_nm, internal_quantum_efficiency_ref, 'o', ...
76      'MarkerFace', 'm', 'MarkerEdge', 'k', 'MarkerSize', 6);
77  plot(wl_nm, IQE, 'k', 'linewidth', 1.2);
78  hold off;
79  set(gca, 'xtick', 0:100:2000);
80  xlabel('Wavelength / nm');
81  ylabel('Internal quantum efficiency');
82  legend('Measured against pyroelectric radiometer', ...
83      'Measured against trap detector', 'Modelled IQE', 'Location', 'North');
84  legend('boxoff');
85
86  % Plot internal quantum efficiency (zoomed)
87  figure;
88  set(gcf, 'color', 'w');
89  plot(M_pyro_resp(:, 1), IQE_pyro, 's', 'MarkerFace', [0.4, 0.4, 1], ...
90      'MarkerEdge', [0.4, 0.4, 1], 'MarkerSize', 6);
91  hold on;
92  plot(wl_meas_nm, internal_quantum_efficiency_ref, 'o', ...
93      'MarkerFace', 'm', 'MarkerEdge', 'k', 'MarkerSize', 6);
```

```
94  plot(UV_wl_nm, IQE_UV.*modelled_QY, 'b--', 'linewidth', 1.2);
95  plot(VIS_wl_nm, IQE_VIS, 'r:', 'linewidth', 1.2)
96  plot(wl_nm, IQE, 'k', 'linewidth', 1.2);
97  hold off;
98  axis([300 500 0.97 1.02]);
99  set(gca, 'xtick', 0:50:2000);
100 xlabel('Wavelength / nm');
101 ylabel('Internal quantum efficiency');
102 legend('Measured against pyroelectric radiometer', ...
103     'Measured against trap detector', 'UV IQE', 'VIS IQE', ...
104     'Modelled IQE', 'Location', 'North');
105 legend('boxoff');
106 % -----
```

3.3.1   Function *fit_ spectral_ reflectance*

Function *fit_ spectral_ reflectance* is used to fit the spectral reflectance model of Section 2.1 to the measured reflectances of the input Excel file.

Listing 3: Function to calculate the spectral reflectance of a trap detector.

```
1   function [thickness_SiO2, modelled_reflectance] = ....
2       reflectanceModel(wl_ref_nm, reflectance_ref, wl_nm, n_Si)
3
4       wl_um = wl_nm/1000;
5
6       % Refractive index of air, Eq. (29)
7       n_air = (0.05792105)./(238.0185 - wl_um.^(-2)) ...
8           + (0.00167917)./(57.362 - wl_um.^(-2)) + 1;
9       % Refractive index of SiO2, Eq. (28)
10      n_SiO2 = sqrt(((0.6961663*wl_um.^2)./(wl_um.^2 - 0.0684043.^2) ...
11          + (0.4079426*wl_um.^2)./(wl_um.^2 - 0.1162414.^2) ...
12          + (0.8974794*wl_um.^2)./(wl_um.^2 - 9.896161.^2)) + 1);
13
14      % ----- Iterative fitting of the thickness of SiO2 layer -----
15      options = optimoptions(@lsqnonlin, 'Algorithm', ...
16          'trust-region-reflective', 'MaxFunEvals', 10000, ...
17          'MaxIter', 10000, 'StepTolerance', 1e-10, ...
18          'OptimalityTolerance', 1e-10, 'FunctionTolerance', 1e-10, ...
19          'Display', 'off');
20      thickness_SiO2 = lsqnonlin(@(x) fit_spectral_reflectance(x, ...
21          wl_ref_nm, reflectance_ref, wl_nm, n_Si), 10, [], [], options);
22      % -----
23
24      theta1 = pi/4;                          % Incident angle
25      theta2 = asin(n_air*sin(theta1)./n_SiO2);   % Angle in SiO2, Eq. (17)
26      theta3 = asin(n_SiO2.*sin(theta2)./n_Si);   % Angle in Si, Eq. (18)
27
28      % ----- Reflectance at 0 degrees -----
29      % Reflection coefficients, Eqs. (7-10)
30      t120 = 2*n_air./(n_air + n_SiO2);
31      r120 = (n_SiO2 - n_air)./(n_SiO2 + n_air);
```

```
32     r230 = (n_Si - n_SiO2)./(n_Si + n_SiO2);
33     t210 = 2*n_SiO2./(n_SiO2 + n_air);
34     % Phase, Eq. (6)
35     b0 = 2*pi./wl_nm.*n_SiO2.*thickness_SiO2.*cos(0);
36     % Reflectance, Eq. (5)
37     r0 = r120 + (t120.*t210.*r230.*exp(-2i*b0))./(1 + r120.*r230.*exp(-2i*b0));
38     R0 = abs(r0).^2;
39     % -----
40
41     % ----- Reflectance of s-polarized radiation -----
42     % Reflection coefficients, Eqs. (13-16)
43     t12s = 2*n_air.*cos(theta1)./(n_air.*cos(theta1) + n_SiO2.*cos(theta2));
44     r12s = (n_air.*cos(theta1) - n_SiO2.*cos(theta2)) ...
45         ./(n_air.*cos(theta1) + n_SiO2.*cos(theta2));
46     r23s = (n_SiO2.*cos(theta2) - n_Si.*cos(theta3)) ...
47         ./(n_SiO2.*cos(theta2) + n_Si.*cos(theta3));
48     t21s = 2*n_SiO2.*cos(theta2)./(n_SiO2.*cos(theta2) + n_air.*cos(theta1));
49     % Phase, Eq. (12)
50     b45 = 2*pi./wl_nm.*n_SiO2.*thickness_SiO2.*cos(theta2);
51     % Reflectance, Eq. (11)
52     rs45 = r12s + (t21s.*t12s.*r23s.*exp(-2i*b45))./(1 + r12s.*r23s.*exp(-2i*b45));
53     RS45 = abs(rs45).^2;
54     % -----
55
56     % ----- Reflectance of p-polarized radiation -----
57     % Reflection coefficients, Eqs. (20-23)
58     t12p = 2*n_air.*cos(theta1)./(n_SiO2.*cos(theta1) + n_air.*cos(theta2));
59     r12p = (n_SiO2.*cos(theta1) - n_air.*cos(theta2)) ...
60         ./(n_SiO2.*cos(theta1) + n_air.*cos(theta2));
61     r23p = (n_Si.*cos(theta2) - n_SiO2.*cos(theta3)) ...
62         ./(n_Si.*cos(theta2) + n_SiO2.*cos(theta3));
63     t21p = 2*n_SiO2.*cos(theta2)./(n_SiO2.*cos(theta1) + n_air.*cos(theta2));
64     % Reflectance, Eq. (19)
65     rp45 = r12p + (t12p.*t21p.*r23p.*exp(-2i.*b45))./(1 + r12p.*r23p.*exp(-2i.*b45));
66     RP45 = abs(rp45).^2;
67     % -----
68
69     % Total reflectance (5 reflections), Eq. (4)
70     modelled_reflectance = R0.*RS45.^2.*RP45.^2;
71 end
```

Listing 4: Fitting of the reflectance model.

```
1 function residual = fit_spectral_reflectance(thickness_SiO2, wl_ref_nm, ...
2     reference_reflectance, wl_Si_nm, n_Si)
3
4     wl_um = wl_ref_nm/1000;
5
6     % Refractive index of air, Eq. (29)
7     n_air = (0.05792105)./(238.0185 - wl_um.^(-2)) ...
8         + (0.00167917)./(57.362 - wl_um.^(-2)) + 1;
9     % Refractive index of SiO2, Eq. (28)
10    n_SiO2 = sqrt(((0.6961663*wl_um.^2)./(wl_um.^2 - 0.0684043.^2) ...
```

```matlab
11          + (0.4079426*wl_um.^2)./(wl_um.^2 - 0.1162414.^2) ...
12          + (0.8974794*wl_um.^2)./(wl_um.^2 - 9.896161.^2)) + 1);
13      % Refractive index of Si at reference wavelengths
14      n_Si = interp1(wl_Si_nm, n_Si, wl_ref_nm, 'pchip');
15
16      theta1 = pi/4;                               % Incident angle
17      theta2 = asin(n_air.*sin(theta1)./n_SiO2);   % Eq. (17)
18      theta3 = asin(n_SiO2.*sin(theta2)./n_Si);    % Eq. (18)
19
20      % ----- Reflectance at 0 degrees -----
21      % Reflection coefficients, Eqs. (7-10)
22      t120 = 2*n_air./(n_air + n_SiO2);
23      r120 = (n_SiO2 - n_air)./(n_SiO2 + n_air);
24      r230 = (n_Si - n_SiO2)./(n_Si + n_SiO2);
25      t210 = 2*n_SiO2./(n_SiO2 + n_air);
26      % Phase, Eq. (6)
27      b0 = 2*pi./wl_ref_nm.*n_SiO2.*thickness_SiO2.*cos(0);
28      % Reflectance, Eq. (5)
29      r0 = r120 ...
30          + (t120.*t210.*r230.*exp(-2i*b0))./(1 + r120.*r230.*exp(-2i*b0));
31      R0 = abs(r0).^2;
32      % -----
33
34      % ----- Reflectance of s-polarized radiation -----
35      % Reflection coefficients, Eqs. (13-16)
36      t12s = 2*n_air.*cos(theta1)./(n_air.*cos(theta1) + n_SiO2.*cos(theta2));
37      r12s = (n_air.*cos(theta1) - n_SiO2.*cos(theta2)) ...
38          ./(n_air.*cos(theta1) + n_SiO2.*cos(theta2));
39      r23s = (n_SiO2.*cos(theta2) - n_Si.*cos(theta3)) ...
40          ./(n_SiO2.*cos(theta2) + n_Si.*cos(theta3));
41      t21s = 2*n_SiO2.*cos(theta2)./(n_SiO2.*cos(theta2) + n_air.*cos(theta1));
42      % Phase, Eq. (12)
43      b45 = 2*pi./wl_ref_nm.*n_SiO2*thickness_SiO2.*cos(theta2);
44      % Reflectance, Eq. (11)
45      rs45 = r12s ...
46          + (t21s.*t12s.*r23s.*exp(-2i*b45))./(1 + r12s.*r23s.*exp(-2i*b45));
47      RS45 = abs(rs45).^2;
48      % -----
49
50      % ----- Reflectance of p-polarized radiation -----
51      % Reflection coefficients, Eqs. (20-23)
52      t12p = 2*n_air.*cos(theta1)./(n_SiO2.*cos(theta1) + n_air.*cos(theta2));
53      r12p = (n_SiO2.*cos(theta1) - n_air.*cos(theta2)) ...
54          ./(n_SiO2.*cos(theta1) + n_air.*cos(theta2));
55      r23p = (n_Si.*cos(theta2) - n_SiO2.*cos(theta3)) ...
56          ./(n_Si.*cos(theta2) + n_SiO2.*cos(theta3));
57      t21p = 2*n_SiO2.*cos(theta2)./(n_SiO2.*cos(theta1) + n_air.*cos(theta2));
58      % Reflectance, Eq. (19)
59      rp45 = r12p ...
60          + (t12p.*t21p.*r23p.*exp(-2i*b45))./(1 + r12p.*r23p.*exp(-2i*b45));
61      RP45 = abs(rp45).^2;
62      % -----
63
64      % Total reflectance (5 reflections), Eq. (4)
```

```
65    modelled_reflectance = R0.*RS45.^2.*RP45.^2;
66
67    residual = (1 - modelled_reflectance./reference_reflectance);
68 end
```

3.3.2 Function *fit_internal_quantum_efficiency*

Function *fit_internal_quantum_efficiency* is used to fit the spectral internal quantum efficiency model of Section 2.2 to the internal quantum efficiencies derived from the responsivities measured for the trap detector.

Listing 5: Fitting the internal quantum efficiency.

```
1  function residual = fit_internal_quantum_efficiency(x, alpha, measured_IQE)
2      Pf = x(1);   % Collection efficiency at the front surface
3      T = x(2);    % Depth of unity collection efficiency
4      Pr = x(3);   % Bulk collection efficiency
5      D = x(4);    % Depth for reaching Pr
6      d = x(5);    % Thickness of the photodiode
7
8      % Spectral internal quantum efficiency model, Eq. (31)
9      modelled_IQE = Pf + (1 - Pf)./(alpha.*T).*(1 - exp(-alpha.*T)) ...
10         - (1 - Pr)./alpha./(D - T).*(exp(-alpha.*T) - exp(-alpha.*D)) ...
11         - Pr.*exp(-alpha.*d);
12
13      residual = (1 - modelled_IQE./measured_IQE);
14 end
```

3.3.3 Function *fit_quantum_yield*

Function *fit_quantum_yield* is used to extend the spectral responsivity of a trap detector to the ultraviolet wavelength region by fitting spectral quantum yield model introduced in Section 2.3 to the quantum yields derived from the responsivities measured for the trap detector.

Listing 6: Fitting the quantum yield in the UV wavelength region.

```
1  function residual = fit_quantum_yield(x, wavelength_nm, measured_QY, ...
2      E_DOS, DOS_electrons, alpha)
3      B = x(1);          % Scaling factor to be fitted
4      deltaE = x(2);     % Energy shift to be fitted
5
6      global h_eV c      % Nature constants
7
8      % Wavelengths converted to the corresponding energies
9      E = (h_eV*c)./(wavelength_nm*1e-9);
10
11     hw = E - deltaE;   % Shifted energy scale
12
13     a = 0.543;         % Lattice constant of Si at room temperature / nm
```

```matlab
14      A = 5.2;          % Empirical constant / eV^3
15      hw0 = 0.062;      % Phonon energy / eV
16      Eg_in = 1.12;     % Energy of indirect transition / eV
17      Eg_d = 3.1;       % Energy of direct transition / eV
18
19      % 3D density of states (DOS) in the conduction band calculated using
20      % pseudopotential method
21      E_DOS_slope = E_DOS(find(E_DOS >= 3.8 & E_DOS <= 4.0));
22      DOS_UV_slope =  DOS_electrons(find(E_DOS >= 3.8 & E_DOS <= 4.0));
23
24      % Effective density of states in the conduction band
25      params = polyfit(E_DOS_slope, log(DOS_UV_slope), 1);
26      tail_fit = exp(polyval(params, E_DOS(find(E_DOS <= 4.0))));
27      DOS_UV_temp = [tail_fit; DOS_electrons(find(E_DOS > 4.0))];
28      DOS_UV = 10*interp1(E_DOS - deltaE, DOS_UV_temp, E, 'pchip');
29
30      % Shifted absorption coefficient at UV
31      alpha_UV = interp1(E - deltaE, alpha, E, 'pchip');
32
33      % Quantum yield to be optimized, Eq. (36)
34      modelled_QY = 1 + ((a^3*B).*(DOS_UV./alpha_UV)./(1 + 105*A./(2*pi) ...
35          .*((hw - Eg_in - hw0).^(1/2))./((hw - 2*Eg_in).^(7/2))) ...
36          .*(E - Eg_d));
37
38      residual = (1 - modelled_QY./measured_QY);
39  end
```

4 Experimental Measurements

4.1 Absolute Laser Responsivity Measurements in Visible and Near-Infrared Spectral Regions

The responsivity calibrations of the working standard silicon trap detectors are made against the reference detector. The wavelengths should cover the visible wavelength range and at least one measurement should be taken near the band gap edge of silicon around 950 nm to ensure the optimal parameter values are achieved when fitting Eq. (31) to the responsivities measured at the wavelengths from 380 nm to 1000 nm. Table 4.1 lists the laser lines currently available at the Metrology Research Institute.

Table 3: Laser lines that are available at the Metrology Research Institute given in air wavelengths.

Gas lasers	
Helium cadmium laser	325 nm, 442 nm
Krypton argon ion laser	476 nm, 483 nm, 488 nm, 496 nm, 514 nm, 521 nm, 531 nm, 568 nm, 647 nm, 676 nm
Green helium neon laser	543 nm
Red helium neon laser	633 nm

Diode lasers	
Ultraviolet diode laser	405 nm
Near-infrared diode laser	933 nm

4.2 Reflectance Measurements

The reflectance of trap detector #1 under test will be measured at different laser wavelengths using the measurement geometry illustrated in Fig. 8. The laser wavelengths can be different from those of the responsivity measurements. First, the input beam power is measured with trap detector #2 and then the geometry is changes so that mirror reflects the input beam to trap detector #1 and the reflected beam is measured with trap detector #2 that was used for measuring the incident beam power. The reflectance of trap detector #1 is calculated from the ratio between the incident laser power and the laser power reflected from the detector surface. The distances between the trap detectors, the mirror, and the laser should be optimized so that the tilt angle of trap detector #1 and the divergence of the laser beam are minimized.
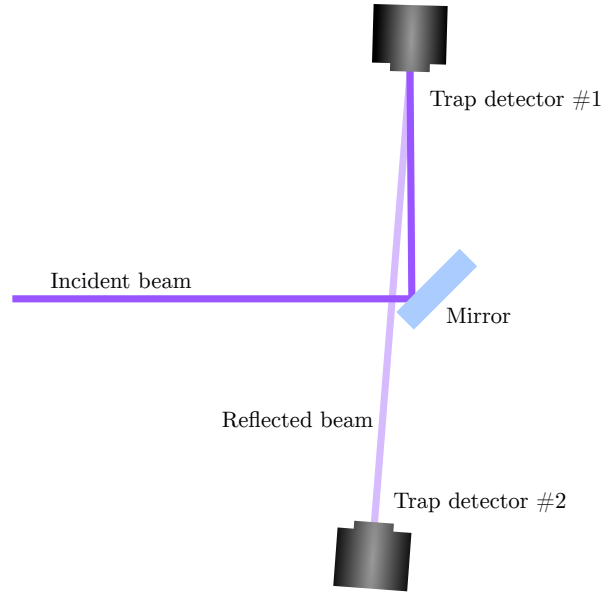
Figure 8: Reflectance measurement geometry.

4.3 Ultraviolet Responsivity Measurements using Pyroelectric Radiometer

The UV responsivity of Si detectors has spectral fine structure and the UV quantum yield model is only approximative. Therefore, we recommend to measure the spectral UV responsivity with the minimum step size of 5 nm against a calibrated pyroelectric radiometer. Pyroelectric radiometers are thermal detectors with spectrally flat responsivity, making them optimal for reference instruments in detector calibration measurements.

References

[1] N. P. Fox, "Trap Detectors and their Properties," *Metrologia* **28**, 197–202 (1991).
DOI: https://doi.org/10.1088/0026-1394/28/3/018

[2] J. Geist, E. F. Zalewski, and A. R. Schaefer, "Spectral response self-calibration and interpolation of silicon photodiodes," *Applied Optics* bf 19, 3795–3799.
DOI: https://doi.org/10.1364/AO.19.003795

[3] T. Dönsberg, M. Sildoja, F. Manoocheri, M. Merimaa, L. Petroff, and E. Ikonen, "A primary standard of optical power based on induced-junction silicon photodiodes operated at room temperature," *Metrologia* **51**, 197–202 (2014).
DOI: https://doi.org/10.1088/0026-1394/51/3/197

[4] T. R. Gentile, J. M. Houston, and C. L. Cromer, "Realization of a scale of absolute spectral response using the National Institute of Standards and Technology high-accuracy cryogenic radiometer," *Applied Optics* **35**, 4392–4403 (1996).
DOI: https://doi.org/10.1364/AO.35.004392

[5] T. Kübarsepp, P. Kärhä, and E. Ikonen, "Interpolation of the spectral responsivity of silicon photodetectors in the near ultraviolet," *Applied Optics* **39**, 9–15 (2000).
DOI: https://doi.org/10.1364/AO.39.000009

[6] J. L. Gardner, "Transmission trap detectors," *Applied Optics* **33**, 5914–5918 (1994).
DOI: https://doi.org/10.1364/AO.33.005914

[7] A. Haapalinna, P. Kärhä, and E. Ikonen, "Spectral reflectance of silicon photodiodes," *Applied Optics* **37**, 729–732 (1998).
DOI: https://doi.org/10.1364/AO.37.000729

[8] R. Goebel, S. Yilmaz, and R. Pello, "Polarization dependence of trap detectors," *Metrologia* **33**, 207–213 (1996).
DOI: https://doi.org/10.1088/0026-1394/33/3/3

[9] R. Goebel and M. Stock, "Nonlinearity and polarization effects in silicon trap detectors," *Metrologia* **35**, 413–418 (1998).
DOI: https://doi.org/10.1088/0026-1394/35/4/33

[10] G. E. Jellison Jr., "Optical functions of silicon determined by two-channel polarization modulation ellipsometry," *Optical Materials* **1**, 41–47 (1992).
DOI: https://doi.org/10.1016/0925-3467(92)90015-F

[11] M. A. Green, "Self-consistent optical parameters of intrinsic silicon at 300 K including temperature coefficients," *Solar Energy Materials & Solar Cells* **92**, 1305–1310 (2008).
DOI: https://doi.org/10.1016/j.solmat.2008.06.009

[12] I. H. Malitson, "Interspecimen comparison of the refractive index of fused silica," *Journal of the Optical Society of America* **55**, 1205–1208 (1965).
DOI: https://doi.org/10.1364/JOSA.55.001205

[13] C. Z. Tan, "Determination of refractive index of silica glass for infrared wavelengths by IR spectroscopy," *Journal of Non-Crystalline Solids* **223**, 158–163 (1998).
DOI: https://doi.org/10.1016/S0022-3093(97)00438-9

[14] P. E. Ciddor, "Refractive index of air: new equations for the visible and near infrared," *Applied Optics* **35**, 1566–1573 (1996).
DOI: https://doi.org/10.1364/AO.35.001566

[15] L. Werner, J. Fischer, U. Johannsen, and J. Hartmann, "Accurate determination of the spectral responsivity of silicon trap detectors between 238 nm and 1015 nm using a laser-based cryogenic radiometer," *Metrologia* **37**, 279–284 (2000).
DOI: https://doi.org/10.1088/0026-1394/37/4/3

[16] J. Geist and C. S. Wang, "New calculations of the quantum yield of silicon in the near ultraviolet," *Physical Review B* **27**, 4841–4847 (1983).
DOI: https://doi.org/10.1103/PhysRevB.27.4841

[17] Y. Okada and Y. Tokumaru, "Precise determination of lattice parameter and thermal expansion coefficient of silicon between 300 and 1500 K," *Journal of Applied Physics* **56**, 314–320 (1984).
DOI: https://doi.org/10.1063/1.333965

[18] R. C. Alig, S. Bloom, and C. W. Struck, "Scattering by ionization and phonon emission in semiconductors," *Physical Review B* **8**, 5565–5582 (1980).
DOI: https://doi.org/10.1103/PhysRevB.22.5565

[19] M. S. Dresselhaus, *Solid State Physics Part II Optical Properties of Solids*, 6th Edition, 2001.

[20] F. Urbach, "The Long-Wavelength Edge of Photographic Sensitivity and of the Electronic Absorption of Solids," *Physical Review* **92**, 1324 (1953).
DOI: https://doi.org/10.1103/PhysRev.92.1324